JTTEE5 4:384-394

Lightweight TiC/Ti Wear-Resistant Coatings for Lightweight Structural Applications

M. Mohanty and R.W. Smith

Lightweight coatings based on titanium and titanium carbides produced by plasma spraying can be used to improve and modify the tribomechanical properties of aerospace structural materials. Although plasma-sprayed WC/Co coatings have been applied with success in many cases, such as primary wear-resistant materials, their high densities preclude their use in applications that mandate reduction in weight. In the present investigation, the sliding wear resistance of plasma-sprayed, metal-bonded TiC coatings on Al 7075 substrates was studied. Coatings containing 50, 70, and 90 vol% TiC in a Ti matrix produced from physically blended powders of Ti and TiC were compared. Metallographic evaluations showed that dense coatings with good bonding to Al 7075 substrates can be obtained. Coatings from commercial purity (CP) Ti powders sprayed in air under atmospheric conditions, however, indicated considerable oxidation of the particles. Under dry sliding conditions, the coefficient of friction (COF) values of the Ti/TiC containing/Al 7075 substrate system were lower than high-velocity oxygen fuel (HVOF) sprayed 75% Cr_3C_2/25%NiCr coatings on steel and were comparable to coatings of WC/Co. Vacuum plasma-sprayed TiC/Ti coatings with 90 vol% TiC also exhibited better wear resistance than HVOF sprayed 75%Cr_3C_2/25%NiCr.

1. Introduction

THE MONOCARBIDES of groups IV, V, and VI metals exhibit exceptional properties, such as high hardnesses, wear resistance, and melting points (Ref 1-5). When such transition metal carbide phases are cemented in a relatively ductile matrix, a combination of high abrasion resistance and toughness is obtained (Ref 3, 4). Cemented titanium carbide based materials were first introduced commercially in 1930 (Ref 6, 7) as the first carbide tools for high-speed cutting of tool steels. The simultaneous development of tungsten carbide based materials (WC-Co) exhibiting strengths 50 to 60% greater than cemented titanium carbide grades, however, caused interest in the use of cemented titanium carbides to wane.

Although efforts were renewed after World War II for the development of titanium carbide based materials, the inability to improve their low impact resistance continued to prohibit their use. Since 1959, when Ford, Inc. introduced (Ref 8, 9) cemented titanium carbide cutting tools with properties superior to cemented tungsten carbide materials, interest in these materials has been growing. Today, titanium carbide based composite materials also show promise for low-weight, high-strength wear-resistant applications at low and high temperatures. Their use as lightweight protective coatings is being considered in aerospace, transportation vehicles, and industrial mechanical equipment, where low mass and/or low inertia designs are required. In the applications, light alloys of aluminum, titanium, and magnesium, as well as polymeric composite materials, such as carbon epoxy, promise high strength, high stiffness at low weight, corrosion protection, and fatigue resistance. Despite their promise, however, these base materials are limited by their inherently low wear resistance. Hence, surface protecting coatings are needed. Due to the inhomogeneous nature of the TiC/metal coatings and the limited temperature capabilities of the base materials, coating processes such as plasma spray can offer the materials flexibility and processing capabilities necessary to provide such coatings. Metal-bonded titanium carbide coatings produced by plasma spraying can thus be a cost effective alternative to enhance and modify the tribomechanical properties of primary aerospace structural materials. Titanium carbide cermet coatings also offer substantial weight savings in such applications by virtue of their reduced density and increased elastic moduli. The properties of titanium carbide and titanium carbide based cermets, processed by conventional powder metallurgy routes or by vapor deposition processes, have been reported (Ref 10, 11). Carbide and nitride based compositions of considerable complexity, e.g. (Ti, Ta, Nb, V, Mo, W) (C, N)-(Ni, Co)-Ti_2AlN, have been developed and even commercialized (Ref 2). Despite this recent surge in research interest in titanium carbide and titanium carbide based cermets, little information is available on their use by the thermal spraying industry.

Thermally sprayed coatings of WC/Co have been widely developed for tribological applications (Ref 12-15). WC/Co has been used as the primary wear-resistant coating material due to its high hardness, acceptable oxidation/corrosion behavior, and excellent compatibility with many iron and nickel based substrate materials. Its choice as a protective coating for lightweight structures is not considered optimal for many of the lightweight materials being considered in aerospace and other transportation vehicles. The high density of such coatings (~13.5 g/cm^3) makes them heavier than necessary and may compromise some lightweight structural designs. Alternatively, the high relative cost of WC/Co (U.S. \$500/m^2 for WC/Co as compared to \$125/m^2 for TiC/Ti for as-coated 250 μm thick coatings assuming 65% coating efficiency) is also a disadvantage to other, less dense wear-resistant coatings such as TiC based hard metals,which are less than 25% the weight and, thus, 25% the cost of WC/Co coatings. Other potential advantages anticipated in us-

Keywords aluminum-based substrates, ball-on-disk tests, composite feedstock, plasma spray process, TiC/Ti composites, wear resistance

M. Mohanty and **R.W. Smith,** Engineering Research Center for Plasma-Aided Manufacturing, Department of Materials Engineering, Drexel University, Philadelphia, PA 19104, USA.

ing such materials in thermal spray processes were recently reviewed (Ref 16, 17). Although thermal spraying of materials such as NiCr/TiC has been reported to be very successful (Ref 18, 19), the substrates used for such coatings have almost always been steel. The application of such coatings on light metal substrates has probably been limited in the thermal spraying industry because of the high temperature effects associated with most spray processes. A majority of light alloys, unlike steel, have low melting points, which prohibits their use by this industry.

As a part of a program to develop lightweight coatings for lightweight structural materials using plasma spraying, the Ti/TiC system was investigated. Coatings of Ti and Ti*X* matrices, where *X* represents Ni, Cr, Al, etc., with TiC reinforcements are being developed using plasma spray processes. Process parameter variations that affect coating structure, adhesion, and cohesion are being evaluated. Coating microstructures, phase analysis, bond-line characterization, and other structural features are being characterized to develop plasma spray coating processes for the materials systems described above. Physical and mechanical properties, such as coefficient of thermal expansion, elastic modulus, and tensile strengths are being measured for optimum coatings. Ball-on-disk sliding wear testing is also

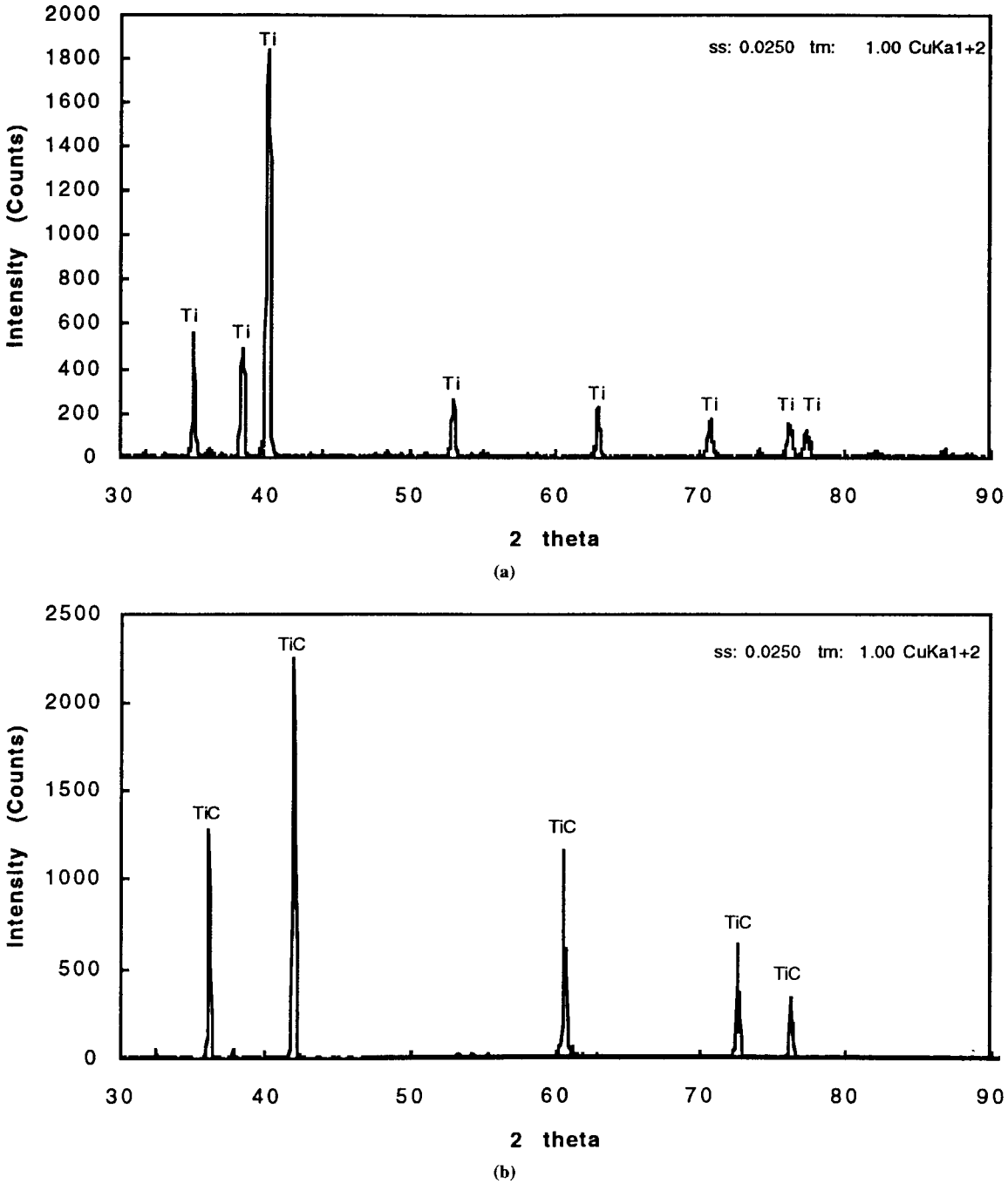

Fig. 1 XRD patterns of feedstock. (a) Titanium powder. (b) Titanium carbide powder

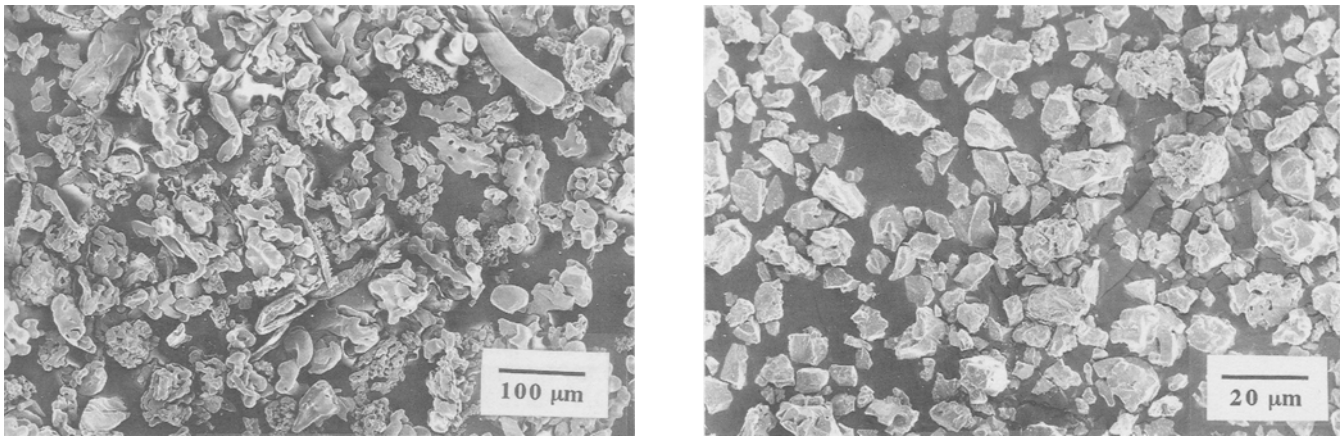

(a) (b)

Fig. 2 Scanning electron micrographs showing the morphology of (a) titanium and (b) titanium carbide powders

Table 1 Properties of the powders used in this investigation

Powder designation	Supplier	Method of manufacture	Particle size	Composition, wt%	Carbide grain size
AMDRY 918-2	Sulzer Pl Tech.	...	–90 μm, +11 μm	99.4 Ti	...
Amperit 570.0	H.C. Starck	..	–23.5, +5.6 μm	TiC	...
JK135	Deloro Stellite	Plasma densified	–45 μm	75% Cr_3C_2/25% NiCr	Prealloyed
Amperit 586.072	H.C. Starck	Agglomerated and sintered	–36 μm, +10 μm	80% Cr_3C_2/20% NiCr	1-2 μm
JK112	Deloro Stellite	Sintered	–45 μm	88% WC/12% Co	1-2 μm

being conducted on selected coating/base material combinations to determine the wear behavior of such material systems.

2. Experimental Procedure

2.1 *Spray Powders*

Commercially available titanium and titanium carbide powders were used in this study. Titanium powder was produced by Sulzer-Metco (SulzerMetco, Westbury, NY) as Amdry 918-2 with a –90 μm + 11μm size range specification. Stoichiometric (1:1) TiC powders, supplied by H.C. Starck (Newton, MA), designated Amperit 570.0, had a particle size range of –23.5 + 5.6 μm. Table 1 indicates the powder designations of the manufacturers, method of manufacture, particle size distribution, and analysis of each powder. The two powders were mechanically blended for 48 h in a 'V'-blender in various proportions to obtain three target composite compositions (Table 2).

As-received powder samples were examined by x-ray diffraction (XRD) analyses using a Siemens D500 (Siemens Analytical X-Ray Instruments, Inc., Madison, WI, USA) x-ray diffractometer to identify the major phases present. The results of scans for the diffractometer set at 40 kV and 30 mA using a CuKα (λ = 1.54°A) radiation source are shown in Fig. 1(a) and (b). The morphologies of the different powders were determined by scanning electron microscopy (Fig. 2). The Ti powders were irregular and exhibited rounded features (Fig. 2a) whereas the TiC powders appeared blocky and angular (Fig. 2b).

Table 2 Composition of the feedstocks and sprayed coatings

Material	Powder composition, vol%	Final coating composition, vol%
Titanium	100 Ti	100 Ti
TiC/Ti	50TiC/50Ti	41TiC/59Ti
TiC/Ti	70TiC/30Ti	70TiC/30Ti
TiC/Ti	90TiC/10Ti	84TiC/16Ti

Note: Final coating composition is measured by image analysis.

2.2 *Substrates*

Al 7075 of the 7*xxx* series contains nominally 5.1 to 6.1 wt% Zn, 2.1 to 2.9 wt% Mg, and 1.2 to 2.0 wt% Cu as the principal alloying elements, and has the greatest response to age hardening of all aluminum alloys, leading to very high strengths (Ref 20, 21). Hence, Al 7075 alloys are widely used in high-strength aircraft structures including extrusions, forgings, and sheets. Another commonly used light alloy is Ti-6Al-4V, which contains nominally 6% aluminum, 4% vanadium, and balance titanium. This alloy combines a minimum tensile strength of 960 MPa with good creep resistance up to 380 °C (Ref 21). Alloys of Ti-6Al-4V are favored for fan blades of jet engines, impellors for pumps, and other forged components. On this basis, Al 7075 and Ti-6Al-4V alloys were chosen as substrates in this investigation. As mentioned earlier, light alloys, such as Al 7075, have a much lower melting point than Ti-6Al-4V alloys, i.e., 635 °C compared to 1660 °C. Since plasma spray processes typically in-

Table 3 Spray parameters

Spray parameters	Coating material					
	Commercially pure Ti	Commercially pure Ti	Commercially pure Ti	50TiC/50Ti	70TiC/30Ti	90TiC/10Ti
Spray system	APS (EPI)	VPS (EPI)	APS (Miller)	VPS (EPI)	VPS (EPI)	VPS (EPI)
Spray distance, mm	76	127	76	150	150	150
Torch type	03CA	03CA	SG100	O3CA	O3CA	O3CP
Anode type	No. 170	No. 170	2083 175	No. 170	No. 170	No. 170
Cathode type	9	9	1083 A129	9	9	9
Arc gas 1 type	Ar (No. 62)	Ar (No. 62)	Ar (No. 62)	Ar (No. 62)	Ar (No. 62)	Ar (No. 62)
Arc gas 1 setting, MPa	0.83	0.76	0.5	0.76	0.76	0.76
Arc gas flow, L/min	66	59	41.5	59	59	59
Arc gas 2 type	He	He	He	H2 (0.009)	H2 (0.009)	H2 (0.009)
Arc gas 2 setting, MPa	0 41	0.38	0.52	0.17	0.27	0.27
Arc gas 2 flow, L/min	28.3	26	18.8	4.7	7.1	7.1
Voltage, V	39	38	43	45	46	46
Current, A	1100	1100	800	1100	1100	1100
Carrier gas	Ar	Ar	Ar	Ar	Ar	Ar
Carrier gas setting, MPa	0 41	0.41	0.41	0.48	0 48	0.48
Carrier gas flow, L/min	8.5	8 5	8.5	8.5	8.5	8.5
Powder feed rate, g/min	25	25	25	40	40	40
Shroud gas	...	...	Ar	...	...	...
Shroud gas flow, L/min	...	...	88 SCFH	...	...	...
Run No	A93789	V93878	A93849	V93961	V93963	V93962

Note: Substrates (Al 7075) were gas (Ar) cooled.

volve high temperatures, the use of Al 7075 as substrates is a problem that merits more study.

2.3 *Coating Procedure*

2.3.1 Equipment

The primary experimental apparatus consisted of an EPI O3CA DC plasma torch (Sulzer, Westbury, NY), a cylindrical steel vacuum chamber, a plasma gas supply system, and a volumetric powder feeder. The direct-current plasma torch was housed in the steel chamber of diameter 1.0 m and length 2.0 m. The plasma torch, rated at 120 kW, consisted of a water-cooled copper anode and a water-cooled tungsten cathode. An EPI 170 anode/nozzle (Sulzer, Westbury, NY) was fitted to the torch and used at atmospheric pressure in air as well as at low pressure (vacuum plasma sprayed, VPS). The power supply for the torch was a Metco Model Type 8MR (Metco Perkin-Elmer, Westbury, NY), with an operating capability up to 80 V and 1100 A.

2.3.2 Coating Process

The blended powder mixtures were dried in a vacuum oven at 100 °C for 10 h prior to spraying. The operating parameters were systematically varied to optimize a coating that was well bonded and had maximum density. Preliminary investigations showed that several key steps had to be taken to obtain satisfactory coatings. These investigations indicated that to minimize segregation and increase deposit efficiencies and coating quality, it was necessary to use a nozzle with internal and upstream powder feed ports and a narrow spray pattern. The spray procedure also involved, as a critical step, cooling of the specimens by Ar gas jets and using a water-cooled copper chill block during the spraying process. Substrate cooling, particularly that of Al 7075, was necessary to prevent melting. Under a given set of spray conditions, the substrate thermal stability determined the specimen standoff distances. The test specimens were sprayed according to the parameters given in Table 3. Surfaces of all specimens were grit blasted using No. 13 alumina grit and were ultrasonically cleaned in alcohol prior to spraying.

For evaluation of the coating quality, Al 7075 coupons, 25 mm × 75 mm in size, were used. For sliding wear tests, Al 7075 disks, 60 mm in diameter and 4 mm thick, were used as substrates. Two disks were coated in a single spray run; they were mounted on the water-cooled, copper chill block that traversed back and forth with the surfaces of the disks normal to the gun nozzle while the gun was traversed vertically during the spraying process.

2.3.3 Microstructural Characterization

Microstructural characterization studies were conducted to determine the coating structure, porosity content, volume fraction of carbides, and presence of secondary phases as related to particular spray conditions. Samples cut from each coated coupon were epoxy mounted in cross section and polished with 120 grit SiC paper using water as a lubricant. Subsequently, three resin bonded diamond disks from TBW Industries were used in sequence to fine grind and polish the samples to a surface finish of <0.3 μm R_a. As the final step in the polishing procedure, a napped polishing cloth saturated with an alumina suspension was used. The suspension medium lightly etches the microstructure. An image analysis system (Image 1.41) coupled to a Zeiss ICM (Zeiss, Carl, Inc., Thornwood, NY) 405 optical microscope served to investigate features such as the distribution of carbides, area fraction occupied by the carbides, and percentage porosity in the coating. Vicker's microhardness measurements were made on polished cross sections of the coatings by indenting at a load of 300 g for 10 s. Ten measurements were taken and

averaged. XRD was used to determine the phases present in the coating.

2.4 *Wear Testing*

Wear tests were carried out under dry sliding conditions in a ball-on-disk configuration using an AMTI Model C (AMTI, Inc., Watertown, MA) wear testing machine according to the ASTM G99-90 (Ref 22) standard. Sliding wear was induced by contacting a rotating coated disk under a load against a stationary 10 mm diam sapphire ball chosen as the counterbody. All tests were performed under dry air environment (at relative humidity <1%). The polished disks were also dried in a vacuum oven at 100 °C for 8 h prior to testing to drive off any moisture that might influence the test results. A computerized data acquisition system, interfaced with the wear tester, recorded the test parameters such as the friction force, the speed, and the coefficient of friction (COF), at a rate of 1 Hz. A twenty-point running average was carried out on the data during its acquisition. The material loss in the wear scars on the coating, caused by the slid-

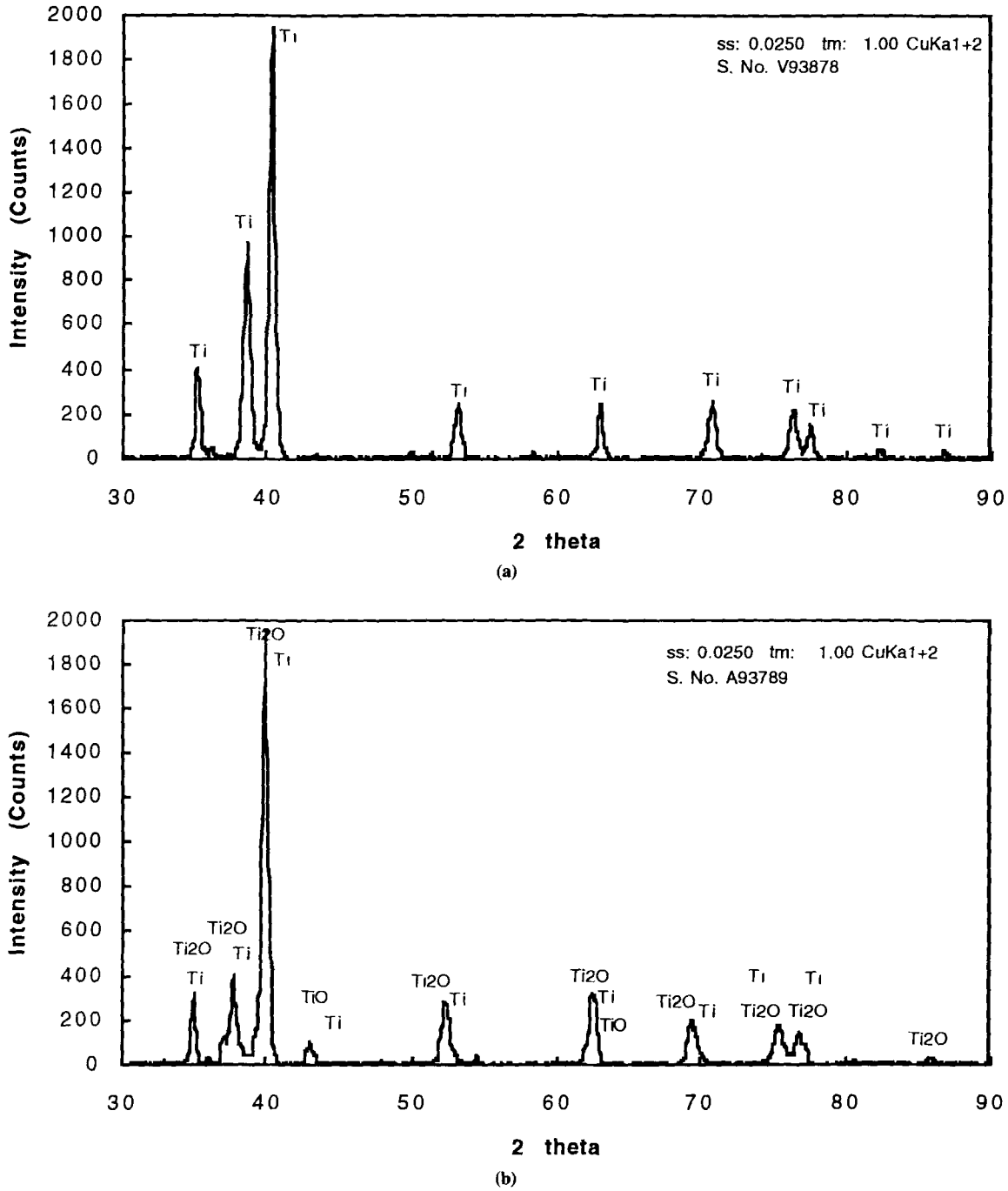

Fig. 3 XRD patterns of (a) low-pressure plasma-sprayed Ti coating and (b) air plasma-sprayed Ti coating

ing of the counterbody against the coating surface, was quantified by the cross-sectional areas of the scars using surface profilometry. For this investigation, a Hommelwerke T20 (Hommel America, Inc., New Britain, CT), a universal surface measurement and evaluation instrument that detects surface irregularities by stylus tracing, was used.

3. Results and Discussion

3.1 *X-Ray Diffraction*

XRD patterns of vacuum and air plasma sprayed (APS) Ti coatings are shown in Fig. 3(a) and (b), respectively. A comparison of the results of the Ti coating obtained in vacuum and in air showed that a considerable amount of titanium reacted with the oxygen in air to form titanium oxide when sprayed under atmospheric conditions, whereas titanium sprayed under vacuum remained essentially unchanged. The primary oxide that appears to have been formed is Ti_2O with lesser amounts of TiO. Higher metal-to-oxygen ratios indicate partial reaction of titanium with oxygen from the air. Thus, the APS coatings probably contain equivalent amounts of both elemental titanium and titanium oxides; therefore, not all Ti transformed to TiO_2.

3.2 *Microhardness*

Table 4 presents the microhardnesses of various coatings. Microhardnesses of the VPS and APS titanium coatings showed significant differences. The low-pressure coating hardness value, averaging around 188 VHN_{300}, was close to that of pure titanium, ~140 VHN_{300} (Ref 23). The slight increase in hardness was probably due to the presence of small amounts of nitrogen and oxygen, typically 2000 to 3000 ppm, dissolved in titanium powder prior to and during spraying, and due to the fine grain structure of the coating. It was difficult to determine any oxides

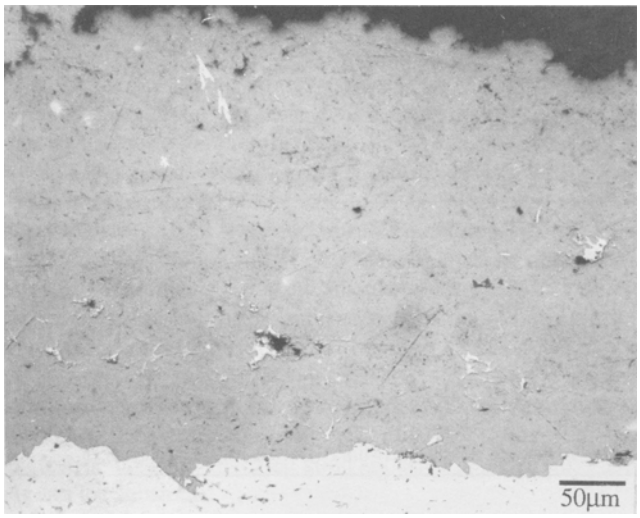

Fig. 4 Optical micrograph of the cross section of low-pressure plasma-sprayed Ti coating

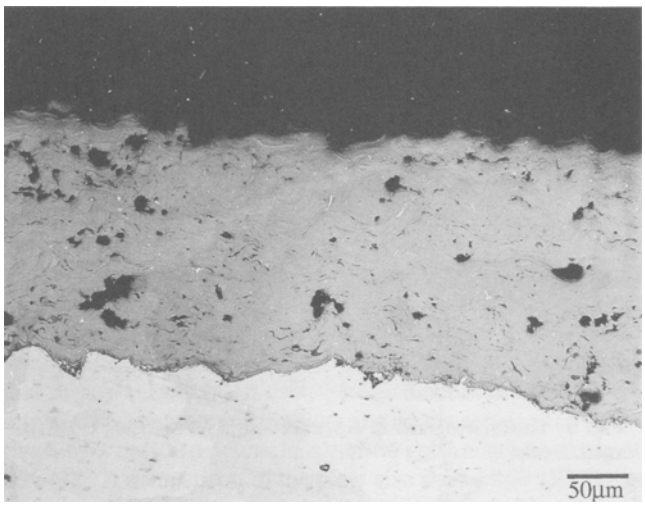

Fig. 5 Optical micrograph of the cross section of APS Ti coating

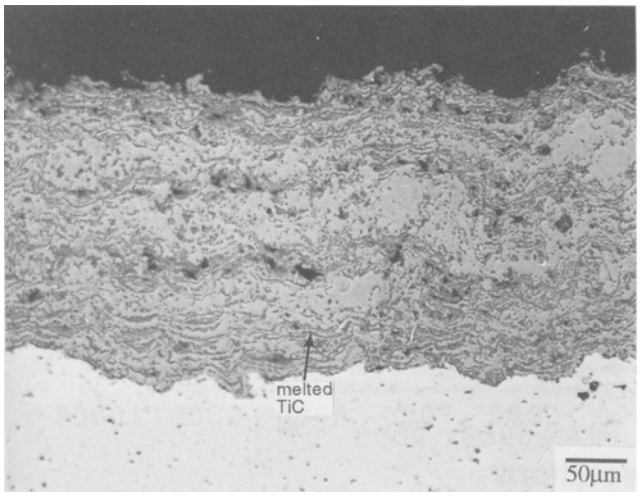

Fig. 6 Photomicrograph of cross section of VPS 50 vol% TiC/50 vol% Ti coating

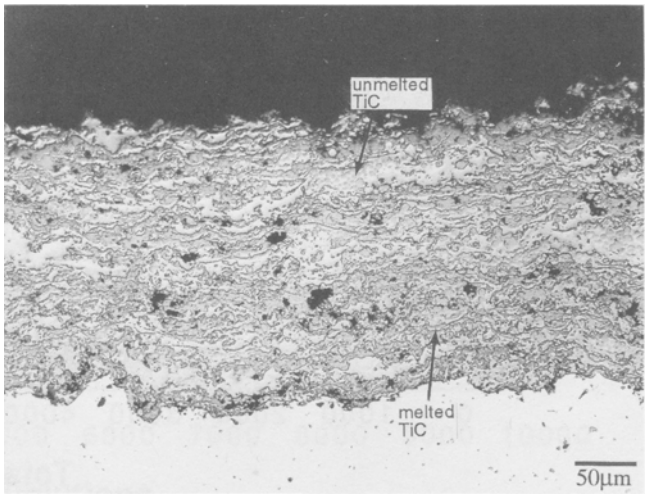

Fig. 7 Photomicrograph of cross section of VPS 70 vol% TiC/30 vol% Ti coating

or nitrides through XRD. However, for the APS titanium coatings, a greater than 300% increase in hardness resulted. This showed the direct influence of oxides formed during Ti powder interactions in air. Although oxidation leads to an increase in hardness, it also has the detrimental effect of decreasing the coating toughness.

A similar, but less dramatic, increase in microhardness with increasing volume percent TiC in Ti was also observed in the VPS TiC/Ti coatings. However, only when the TiC content was increased to 90 vol%, could coating hardness values greater than 500 VHN_{300} be obtained. This demonstrated that a threshold level of TiC phase (>70 vol%) was needed before a substantial increase in coating hardness was realized. Investigations are continuing to evaluate the air plasma spraying of such TiC/Ti coatings. Preliminary results indicate that dense, low oxide content and well-reinforced TiC/Ti coatings are difficult to produce using normal air plasma spraying. It is postulated that this is due to a lack of wetting of TiC by molten titanium particles because of oxidation of the surface of the titanium particles.

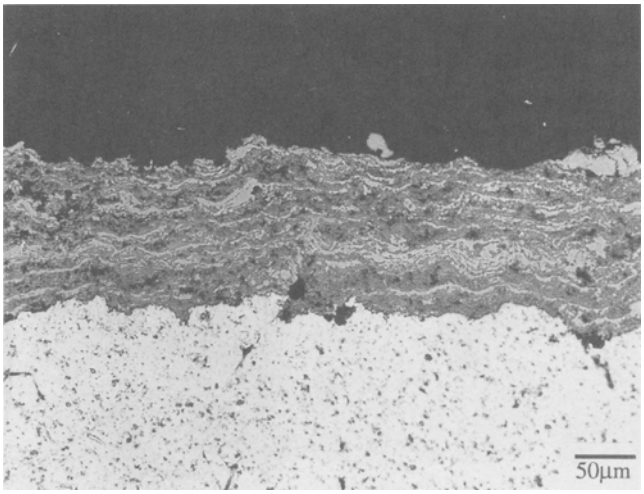

Fig. 8 Photomicrograph of cross section of VPS 90 vol% TiC/10 vol% Ti coating

3.3 *Coating Structure*

An optical micrograph of a VPS Ti coating, shown in Fig. 4, shows a dense and clean microstructure. Isolated pores seen in the coating structure are due to the use of coarse Ti powders. (Coarse titanium powders were used because powders below 30 μm are pyrophoric and thus hard to handle.) The coating also appears to be very well bonded to the Al 7075 substrate.

Figure 5 illustrates the structure of an APS titanium coating. Although the microstructure exhibits a fairly dense (>95%) coating by comparison to the VPS coating of Fig. 4, faint profiles of a lamellar structure indicating contamination due to oxidation of the splats could be distinguished. High hardness values and XRD analyses confirmed these observations. These high hardness values also indicated a decrease in ductility. It is expected that APS titanium, although dense and hard, would not exhibit good wear behavior due to its low toughness. In general it is believed that a tough, lower hardness metallic binder, such as titanium, is preferred for a high volume percent TiC rein-

Table 4 Coating microhardness

Coating	Microhardness, VHN at 300 g	Standard deviation, VHN at 300 g
CP Ti (APS/EPI)	975	175
CP Ti (VPS/EPI)	211	46
CP Ti (APS/Shroud) (a)	625	136
50TiC/50Ti	327	76
70TiC/30Ti (VPS)	437	118
90TiC/10Ti (VPS)	842	210

(a) Miller thermal SG100 gun (Miller Thermal, Inc., Appleton, WI).

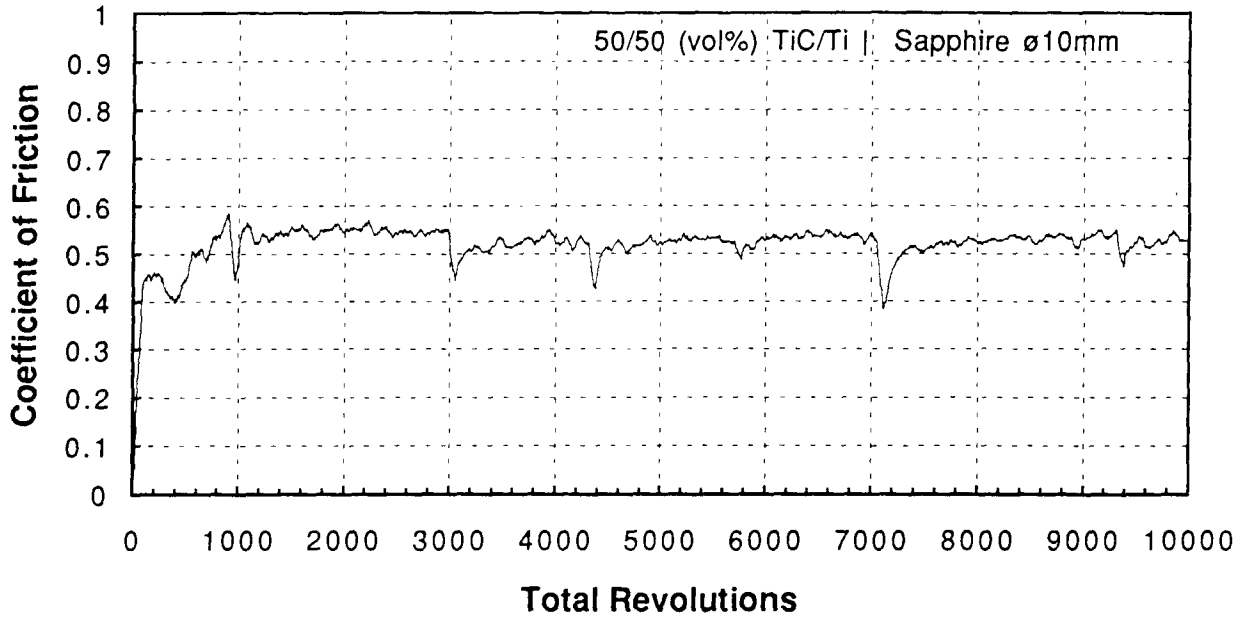

Fig. 9 Average coefficient of friction vs revolutions for low-pressure plasma-sprayed 50 vol% TiC/50 vol% Ti coating. Load = 30 N; sliding speed = 0.44 m/s; rpm = 247; wear track radius = 17 mm

forced coating. The coating also showed relatively good bonding to an Al 7075 substrate. Again, some regions of poor bonding observed may be attributed to oxidation of particles. Because the goal of this research program is to coat lightweight structural materials with lightweight coatings, observation of a good bonding is an encouraging result.

Figures 6, 7, and 8 show optical micrographs of three VPS coatings with 50, 70, and 90 vol% TiC (mechanically mixed), respectively. Such coatings were proposed to be potential replacements for WC/Co coatings on aluminum, titanium, and carbon-epoxy substrates. Coatings with densities greater than 98% were obtained. The coatings showed some degree of layering, which resulted in Ti-rich layers and TiC-rich layers and suggested some segregation of particles in flight when a mechanically blended powder was sprayed. In this case, even though the densities of the Ti and TiC are similar (4.51 g/cm^3 and 4.94 g/cm^3, respectively), the differences in particle size and morphology leads to segregation. This was also apparent by the decrease in coating thickness as the volume percent TiC increased for the same powder feed rate because the smaller and lighter TiC particles were segregated to a greater extent than the larger and heavier Ti particles. Despite the known disadvantages of mechanical mixtures, more than 80% of the carbides in the starting mixtures were retained in the coatings, as shown in Table 2. The coating structures also indicated melting of the carbides, shown labeled in Fig. 6 and 7. In fact, a few isolated regions were evident where individual unmelted TiC particles can be seen. Overall, however, the scale of layering of carbides was fine and uniform. Good cohesion was observed in all the titanium splats and all other interphase splat boundaries. Moreover, some level of metallurgical bonding and changes to the TiC phases can be seen at the TiC/Ti interface regions. The strongest interactions suggested by optical examination were in the highest TiC content coatings (>90 vol% TiC). See Fig. 8. The microstructures also revealed good adhesion between this coating and the substrate.

During spraying, the Al 7075 substrate had to be gas cooled in addition to being mounted on a water-cooled, copper chill block because in the preparatory runs the low melting Al 7075 substrate melted. On the other hand, plasma spraying of Ti on Ti-6Al-4V substrate did not require gas cooling. In all other respects, the coatings obtained on Ti-6Al-4V substrates were very similar to the titanium coatings on Al 7075; hence, they were not reported here. Thus, further investigations are needed to determine or estimate the substrate temperatures under different spraying conditions. As Table 4 indicates, the blended TiC/Ti powders were sprayed with a higher enthalpy gas mixture, Ar and H_2 (Ref 24), so that the carbides could be melted, whereas dense coatings of Ti could be obtained using a lower enthalpy Ar and He gas mixture. A lower enthalpy gas mixture, such as Ar and He, may be used to spray TiC reinforced coatings if the precursor powders are composites instead of mechanical blends.

3.4 *Sliding Wear*

The friction plots for the three TiC/Ti combinations are shown in Fig. 9-11. Figures 12 and 13 show comparative friction data for HVOF (Jet Kote II) sprayed JK112 (88 wt% WC/12 wt% Co) and JK135 (75 wt% Cr_3C_2/25 wt% NiCr) coatings tested under the same conditions. The friction plots of the three TiC/Ti coatings reveal that the instantaneous cyclic variations of COF were highest at the lowest volume fraction of TiC (50 vol%) (Fig. 9) and lowest at the highest volume fraction of TiC (90 vol%) (Fig. 11). These changes resulted from variation in the frictional forces and occurred when the reinforced carbide or matrix material was continuously removed from the surface. Therefore, if the initial metal matrix is easily removed or transferred selectively, hard carbides are released from the matrix; this in turn results in an even greater amount of material removal. This suggests that titanium as a matrix serves as an effective binder only at amounts less than 30 vol% and is best only at 10 vol%. A comparison of the plots also shows that TiC/Ti ex-

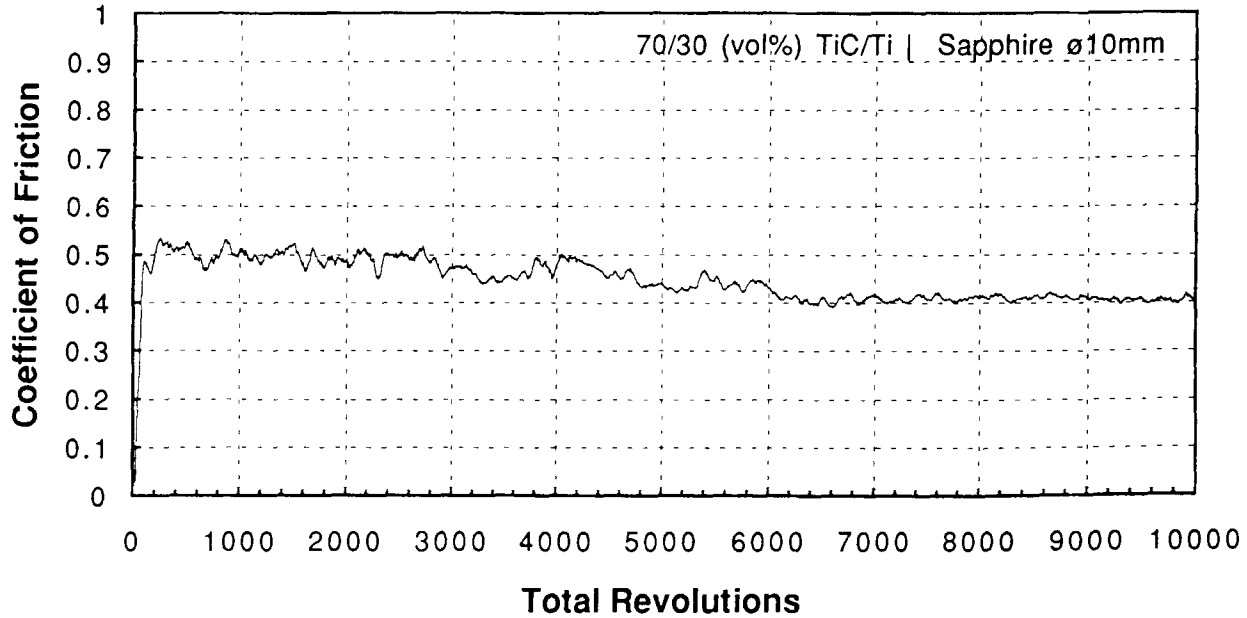

Fig. 10 Average coefficient of friction vs. revolutions for low-pressure plasma-sprayed 70 vol% TiC/30 vol% Ti coating. Load = 30 N; sliding speed = 0.44 m/s; rpm = 247; wear track radius = 17 mm

hibited lower COF values than the alternate 75 wt% Cr_3C_2/25 wt% NiCr HVOF coatings and values comparable to WC/Co coatings. These low COF values for TiC/Ti show promise for TiC reinforcements to achieve lower COF values and thus reduce energy losses.

Figure 14 summarizes the wear track cross-sectional areas for the two previously listed commercial thermal spray coatings and the TiC/Ti coatings. For the VPS TiC/Ti coatings, there is over an order of magnitude decrease in wear as the volume fraction TiC is increased from 50 to 90%. This result supports the earlier assumption that the metallic binder controls wear only at higher volume fractions of Ti. Thus, although the TiC phases appeared to be well bonded to the Ti, a greater level of wetting between the carbide and the metal binder is needed. If the binder-carbide interaction is improved, for example, by modifying the binder material, then a higher amount of binder metal can be used without substantial change in any property. Figure 14 also shows the exceptional wear resistance of HVOF sprayed

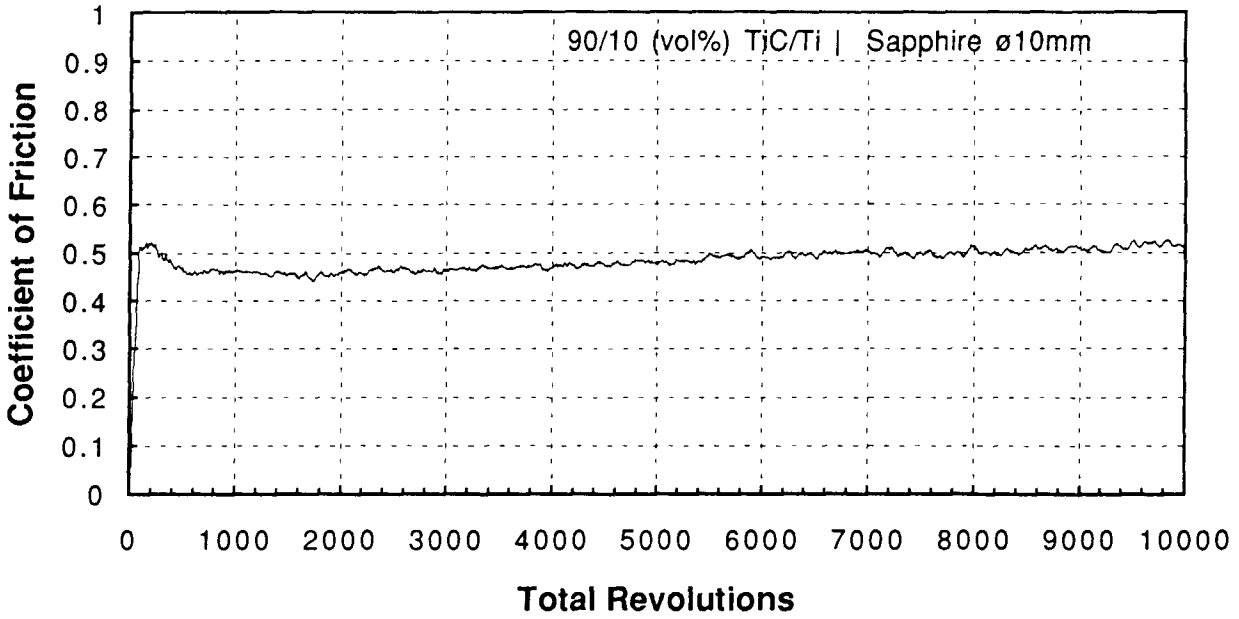

Fig. 11 Average coefficient of friction vs. revolutions for low-pressure plasma-sprayed 90 vol% TiC/10 vol% Ti coating. Load = 30 N; sliding speed = 0.44 m/s; rpm = 200; wear track radius = 21 mm

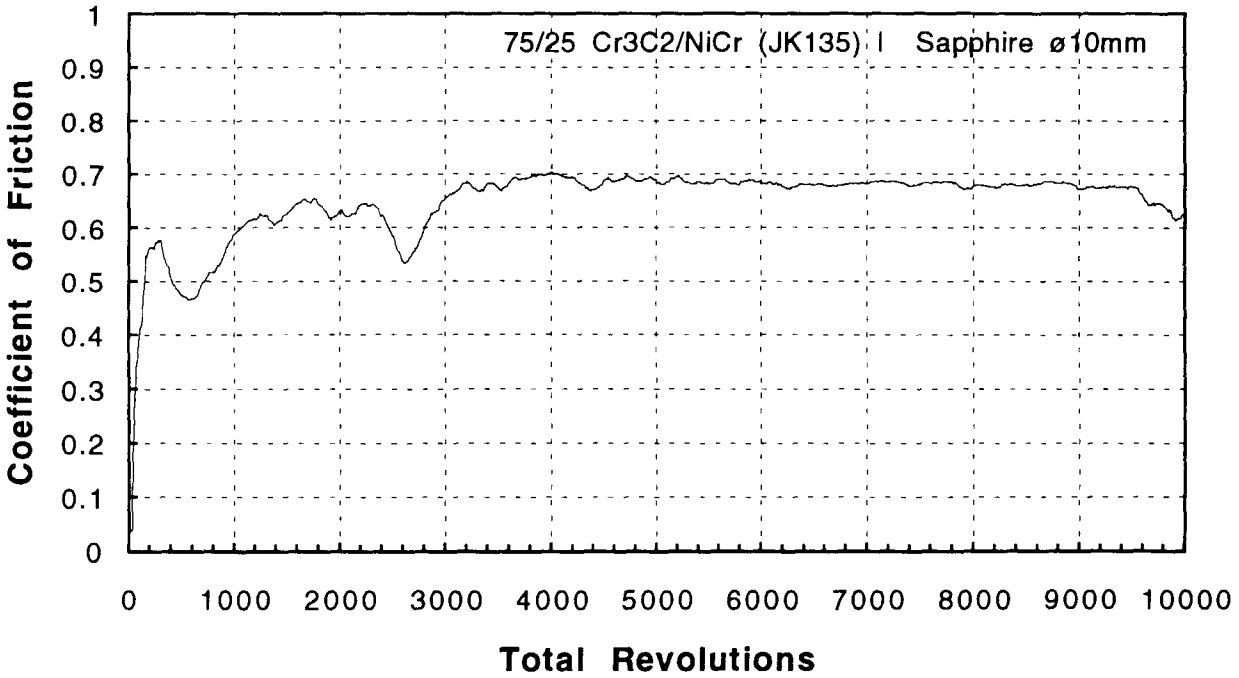

Fig. 12 Average coefficient of friction vs. revolutions for HVOF sprayed 75 Cr_3C_2/25 NiCr coating. Load = 30 N; sliding speed = 0.44 m/s; rpm = 200; wear track radius = 21 mm

WC/Co coating under these test conditions. On the other hand, VPS TiC/Ti coatings with 90 vol% TiC showed better wear resistance than the HVOF (Jet Kote II) (Deloro, Stellite, Inc., Goshen, IN) sprayed 75 wt% Cr_3C_2/25 wt% NiCr coating. This indicated that TiC-based coatings show promise in many applications and may also substitute for WC/Co in less aggressive wear conditions.

4. Conclusions

4.1 *Coating Structures*

Investigations have shown that controlled atmospheres are needed to deposit titanium binder phases and TiC/Ti coatings to

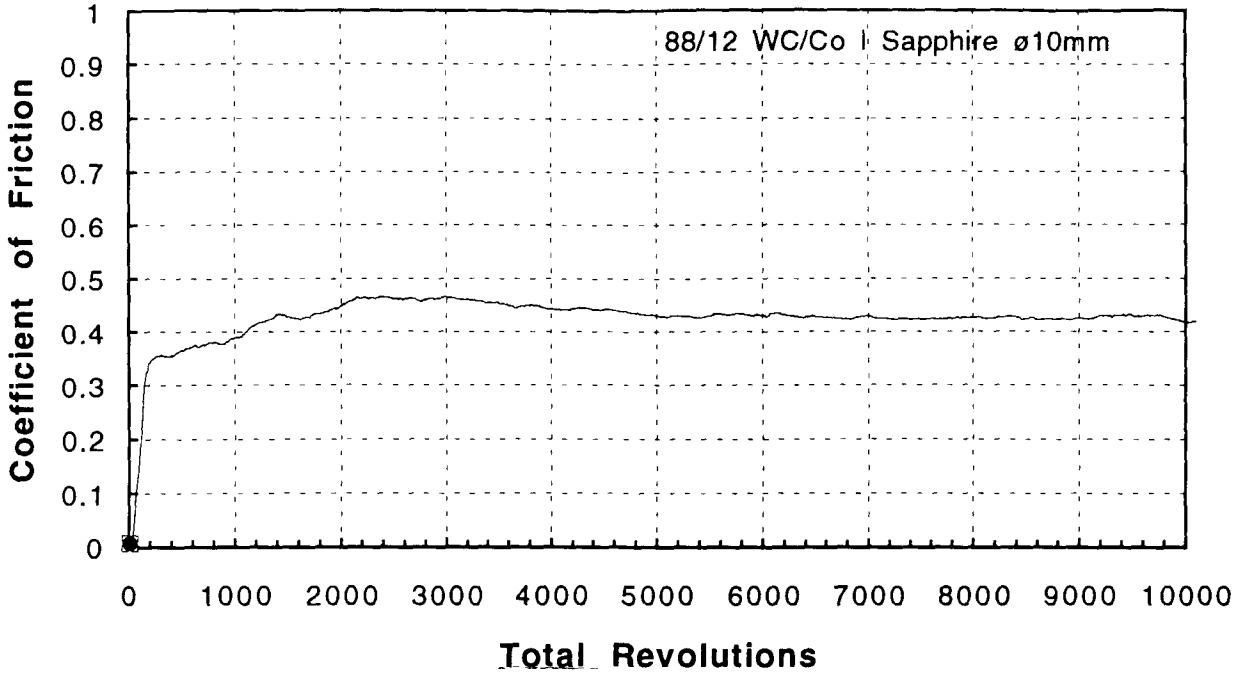

Fig. 13 Average coefficient of friction vs. revolutions for HVOF sprayed 88 WC/12 Co coating. Load = 30 N; sliding speed = 0.44 m/s; rpm = 322; wear track radius = 13 mm

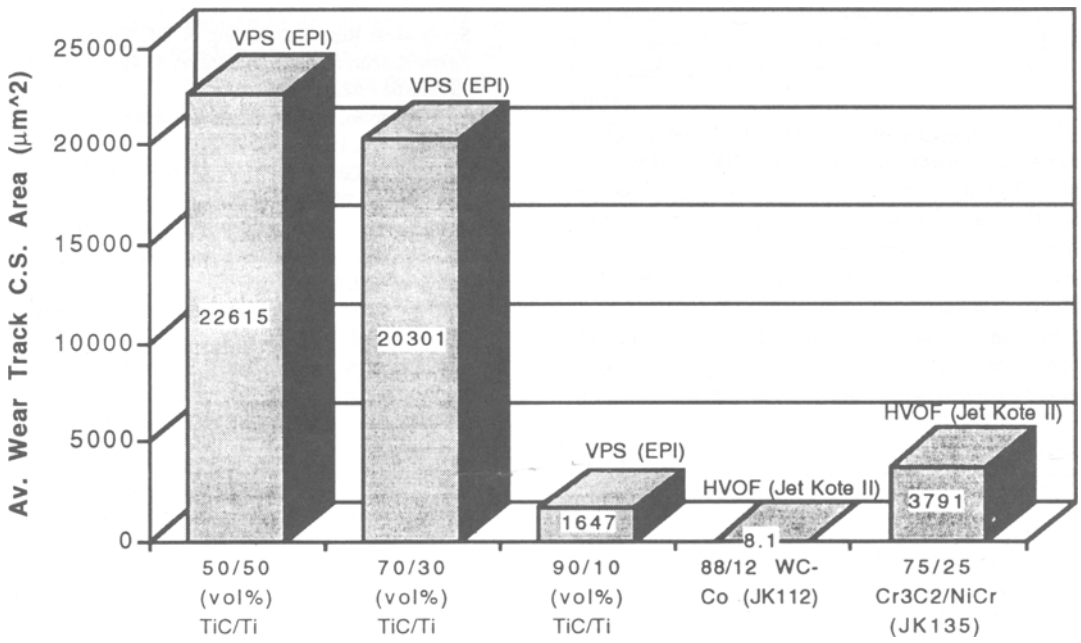

Fig. 14 Summary of total wear from ball-on-disk testing of thermally sprayed coatings Load = 30 N; sliding speed = 0.44 m/s; counterbody = Ø(diameter) 10 mm sapphire, revolutions = 10,000

minimize the degrading effects of reaction with oxygen in the atmosphere. Vacuum plasma spraying of TiC/Ti produced deposits of density greater than 98%. Relatively good intersplat and interphase cohesion and good coating-substrate bond integrity (as observed by optical microscopy) were achieved. Even though mechanical mixing leads to a small extent of layering, over 80% of the initial TiC was retained in the coatings. Mechanical mixing, however, appears to lead to segregation during spraying and lower deposit efficiencies. The use of composite titanium carbide/metal powders is likely to reduce such problems.

4.2 *Sliding Wear*

Comparison of the 90 vol% TiC/Ti coatings on aluminum to Cr_3C_2/NiCr coatings on steel showed that the TiC/Ti coatings performed better under similar conditions, which demonstrated that TiC-based coatings onto aluminum have a high potential as wear-resistant coatings. However, it was also found that titanium matrices at high volume fractions were not effective binders, which suggested that the Ti binder might be modified. In addition, because pure titanium has low oxidation resistance under sliding wear conditions, other titanium alloys or metallic binders need to be investigated. These investigations are planned for the next phase of this work.

Acknowledgments

The authors acknowledge the support of the National Science Foundation (Contract No. ECD-8721545) under the Engineering Research Center for Plasma-Aided Manufacturing at the University of Wisconsin-Madison and University of Minnesota, Minneapolis and their industrial members for this research. The authors would also like to thank the Center for the Plasma Processing of Materials at Drexel University and its Industrial Consortium for their continuing support and the Center's continuing support from the Ben Franklin Partnership of Southeastern Pennsylvania.

References

1. R.K. Viswanadham, B. Sprissler, W. Precht, and J.D. Venables, The Effect of V/Ti Ratio on the Partitioning of Mo in (V,Ti)C + (Ni,Mo) Cemented Carbides, *Metall. Trans. A*, Vol 10 (No. 5), 1979, p 599-602
2. J.L. Ellis and C.G. Goetzel, Cermets, *ASM Handbook*, Vol 2, ASM International, 1990, p 978-1007
3. A.T. Santhanam, P. Tiernen, and J.L. Hunt, Cemented Carbides, *ASM Handbook*, Vol 2, ASM International, 1990, p 950-977
4. H.J. Scussel, Friction and Wear of Cemented Carbides, *ASM Handbook*, Vol 18, ASM International, 1992, p 795-800
5. R.W. Stevenson, Cemented Carbides, *ASM Handbook*, Vol 7, ASM International, 1992, p 773-783
6. P. Swarzkopf and R. Kieffer, *Cemented Carbides*, MacMillan, 1960, p 7-9
7. D. Moskowitz and M. Humenik, Jr., Cemented Titanium Carbide Cutting Tools, *Modern Developments in Powder Metallurgy*, Vol 3, *Developments and Future Prospects*, H.H. Hausner, Ed., Plenum Press, 1966, p 83-93
8. *Production*, Vol 43 (No. 5), 1959, p 99
9. E.J. Egan, Jr., Titanium Carbides Wear Better, *Iron Age*, Vol 183 (No. 12), 1959, p 101
10. H.E. Exner, Physical and Chemical Nature of Cemented Carbides, *Int. Met. Rev.*, Vol 24 (No. 4), 1979, p 149-173
11. V.K. Sarin and J.N. Lindstorm, The Effect of Eta Phase on the Properties of CVD TiC-Coated Cemented Carbide Cutting Tools, *J. Electrochem. Soc.*, Vol 126 (No. 4), 1979, p 1281-1287
12. S. Rangaswamy and H. Herman, Metallurgical Characterization of Plasma Sprayed WC-Co Coatings, *Advances in Thermal Spraying*, Pergamon Press, 1986, p 101-107
13. Z.Z. Mutasim, R.W. Smith, and L. Sokol, Vacuum Plasma Spray Deposition of WC-Co, *Thermal Spray Research and Applications*, T.F. Bernecki, Ed., ASM International, 1991, p 165-169
14. T.N. Rhys-Jones, Thermally Sprayed Coating Systems for Surface Protection and Clearance Control Applications in Aero Engines, *Surface and Coatings Technology*, Vol 43-44 (No. 1-3), 1990, p 402-415
15. D. Ghosh, D. Lamy, T. Sopkow, and I. Smugga-Otto, The Effects of Plasma Spraying Parameters and Atmosphere on the Properties and Microstructure of WC-Co Coatings, *Conf. Advanced Mater.: Meeting the Economic Challenge*, (Toronto, Canada), Society for the Advancement of Material and Process Engineering, 1992, T28-T42
16. E. Lugscheider, Plasma Spraying for Wear Applications, *Thermal Spray Advances in Coatings Technology*, D. Houck, Ed., ASM International, 1988, p 105-122
17. R.W. Smith, Reactive Plasma Spray Forming for Advanced Materials Synthesis, *Powder Metall. Int.*, Vol 25 (No. 1), 1993, p 9-16
18. R.W. Smith, D. Gentner, E. Harzenski, and T. Robisch, The Structure and Properties of Thermally Sprayed TiC Particulate Reinforced Steel and Nickel-Chromium Alloy Powders, *Thermal Spraying*, Vol 1, The Welding Institute, 1989, p 95.1-95.3
19. R.W. Smith, E. Harzenski, and T. Robisch, High Velocity Oxy-Fuel Spray Wear Resistant Coating of TiC Composite Powders, *Thermal Spray Research and Applications*, D. Houck, Ed., ASM International, 1991, p 617-623
20. L.F. Mondolfo, Ch 4-4, *Aluminum Alloys: Structure and Properties*, Butterworths, 1976, p 842-882
21. I.J. Polmear, Ch 3 and 6, *Light Alloys, Metallurgy of the Light Metals*, 2nd ed., Edward Arnold, 1989
22. "Standard Test Method for Wear Testing With a Pin-on-Disk Apparatus," G99-90, *1991 Annual Book of ASTM Standards*, Vol 03.02, Section 3, ASTM, 1991, p 387-391
23. C.J. Smithells, *Smithells Metals Reference Book*, E.A. Brandes and G.B. Brook, Ed., 7th ed., Butterworths, 1991, p 21(1)-22(164)
24. M. Vardelle, A. Vardelle, and P. Fauchais, Spray Parameters and Particle Behavior Relationships During Plasma Spraying, *J. Therm. Spray Technol.*, Vol 2 (No. 1), March 1993, p 79-91